Journal of Crystal Growth 477 (2017) 65–71

Contents lists available at ScienceDirect

Journal of Crystal Growth

journal homepage: www.elsevier.com/locate/crys

Characterization of antimonide based material grown by molecular epitaxy on vicinal silicon substrates *via* a low temperature AlSb nucleation layer

J.B. Rodriguez [a,b,*], L. Cerutti [a,b], G. Patriarche [c], L. Largeau [c], K. Madiomanana [a,b], E. Tournié [a,b]

[a] *Université de Montpellier, IES, UMR 5214, F-34000 Montpellier, France*
[b] *CNRS, IES, UMR 5214, F-34000 Montpellier, France*
[c] *CNRS-C2N, Université Paris-Saclay, F-91460 Marcoussis, France*

ARTICLE INFO

Article history:
Available online 5 April 2017
Communicated by T.F. Kuech

Keywords:
A1. Heteroepitaxy
A1. X-ray diffraction
A2. Molecular beam epitaxy
B1. Antimonides
B1. Silicon substrate
B2. Semiconducting III–V materials

ABSTRACT

We report on the characterization of GaSb layers grown on silicon substrates using an AlSb nucleation layer. In particular, we investigate the influence of the AlSb layer thickness when this nucleation layer is grown at low temperature (400 °C). X-ray diffraction techniques, atomic force microscopy and transmission electron microscopy were used to characterize the material properties. We demonstrate that there exists a correlation between the micro-twin density, the surface roughness and the broadening of the ω-scan GaSb peaks. Moreover, the AlSb thickness has a strong influence on the micro-twin density, and must be carefully optimized to improve the GaSb quality.

1. Introduction

Integration of III–V semiconductors onto silicon substrates to combine the advantages of these two complementary technologies will open new photonic and electronic functionalities. Even if the heterogeneous integration, *i.e.* wafer bonding, allowed demonstrating state-of-the-art performance devices [1,2], this technology faces issues such as the difference of wafer size, the loss of material during processing, etc. On the other hand, over the last decade important efforts have been dedicated to the direct growth of III–V semiconductors on Si to overcome the limitation of wafer bonding. Nonetheless, the large lattice mismatch between most III–Vs and silicon combined with the polar on non-polar interface generally results in a large density of both linear and planar defects. A better understanding of their formation mechanisms is therefore of prime interest in order to grow the high crystallographic quality layers needed for the realisation of practical devices. This is particularly relevant for the integration on Si of III-Sb semiconductors because of their unique properties for the realisation of high performance high-electron-mobility transistors (HEMT) and optoelectronic devices [3,4]. The properties of the growth of GaSb on Si have been extensively studied particularly by high-resolution transmission electron microscopy (HRTEM) [5–8], but only few studies were reported on the relationship between the growth conditions during nucleation and the defects morphology and density [9,10]. We previously demonstrated the influence of the Si surface preparation on the formation of defects in the epilayer [11], and we have investigated the influence of the thickness and the growth temperature of the AlSb nucleation layer on the epilayer quality [12]. In particular, we have shown that at high nucleation temperature, the broadening of the GaSb peak measured on ω-scans resulted from the imperfection of the dislocation array at the interface between silicon and the III–V material [12].

In this paper, we focus on the properties of GaSb layers grown using an AlSb nucleation layer deposited at low temperature (400 °C). In contrast to what occurs at high nucleation temperature, we show that the micro-twins (MTs) are the main defects determining the surface roughness as well as the broadening of the ω-scans GaSb peaks.

2. Experimental details

The samples studied in this paper were grown by molecular beam epitaxy (MBE) on Si (001) substrates having an offcut of 6° toward the [110] direction. Prior to each growth run, the substrate was first prepared using an *ex-situ* preparation scheme described in Ref. [11], and based on several cycles of HF dip and O_2 plasma

* Corresponding author at: Université de Montpellier, IES, UMR 5214, F-34000 Montpellier, France.

E-mail address: rodriguez@ies.univ-montp2.fr (J.B. Rodriguez).

http://dx.doi.org/10.1016/j.jcrysgro.2017.04.003
0022-0248/

treatments. Ellipsometry, performed after each step during the substrate preparation, allowed monitoring surface cleaning and de-oxidation. The substrate was then quickly loaded into the MBE. Fig. 1 shows the substrate temperature evolution and shutter sequence used before and at the beginning of the growth. Substrate temperature was monitored using a standard pyrometer. The substrate is first heated to 800 °C inside the MBE growth chamber to remove residual oxide and impurities. The temperature is then decreased down to the nucleation temperature (400 °C). An AlSb nucleation layer with a thickness comprised between 1 and 50 monolayers (MLs) is then deposited, and immediately covered by a 50 nm thick GaSb layer grown at the same temperature. The gallium shutter is then closed, the substrate temperature set to 450 °C under antimony (Sb) flux, and a thicker (450 nm) GaSb buffer layer and a quantum well (QW) structure are finally grown. The 500 nm thick QW region is embedded into two 20 nm thick AlSb layers, and comprises three 10 nm thick GaInAsSb QWs and 20 nm thick AlGaAsSb barrier layers. The structure is finally capped by a 20 nm thick GaSb layer.

X-ray diffraction measurements were carried out using a PANalytical X'Pert3 MRD equipped with a PIXcel1D linear detector, and an X-ray tube providing Cu Kα1 radiation. The ω-scans were recorded with a four bounce asymmetric Ge (220) mono-chromator and the PIXcell1D in the open detector configuration which corresponds to a 2.5° aperture angle. The pole figures were measured using a Ni filter placed on the incident beam path, without the mono-chromator. The roughness and morphology of the samples' surface were characterized by atomic force microscopy (AFM).

3. Results and discussion

3.1. In-plane pole figure analysis

Fig. 2 presents the pole figures measured for five samples, having an AlSb nucleation layer grown at low temperature with thicknesses of 1, 4, 17, 30 and 50 MLs respectively. The radial and angular axis on these graphs correspond to the inclination of the sample surface with respect to the scattering plane (χ) and the rotation of the sample around its surface normal (ϕ) respectively. The sample is initially aligned for $\phi = 0°$ with the X-ray beam in the [1 1 0] direction of the sample. The ω and 2θ angles of the diffractometer are optimized on a GaSb (1 1 1) diffraction peak and remain constant during the measurement. ϕ-scans were then recorded with a 0.5° resolution, for each χ between 0 and 70° by 1° steps. On each graph, the four most intense peaks at large χ and ϕ = 0, 90, 180 and 270° correspond to the diffraction on these GaSb {1 1 1} planes. As expected, these planes have a fourfold

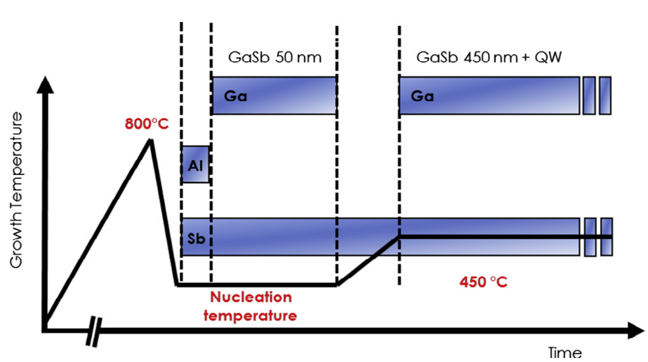

Fig. 1. Evolution of the substrate temperature during substrate annealing, nucleation layer and buffer growth.

symmetry, and are inclined at about 55° to the (0 0 1) planes. The presence of MT in the structure leads to the creation of additional (1 1 1)-type planes having a similar symmetry, but a smaller inclination of 15.9°. MT peaks around $\chi \sim 15°$ are clearly observable on all measurements of this sample set, with the exception of the sample comprising 4 MLs of AlSb as a nucleation layer, for which the MT peaks are difficult to extract from the background. Some ϕ shifts and diffraction distortions of the (1 1 1) and MT peaks are also visible, mainly in the ϕ = 90 and 270° directions, and are due to the linear source we have used and to the large substrate offcut. The MT peaks at ϕ = 90 and 270° have an almost equivalent intensity, indicating an even distribution of the MT in these two directions, perpendicular to the substrate offcut.

By contrast, there is a strong anisotropy of the MT distribution in the directions parallel to the offcut (ϕ = 0 and 180°). The peak corresponding to $\phi = 0°$ has an intensity comparable to the ones on $\phi = 90°$ and 270°, whereas the peak in the opposite direction ($\phi = 180°$) is almost nonexistent. This interesting feature, which was extensively studied by Devenyi et al. [13], is a clear indication that the offcut plays a significant role on the MT density. Fig. 2.f presents the ϕ-scans measured around 250° for the five samples when $\chi = 15.9°$ to have a better insight on the MT peak intensity differences. Again, nice peaks are resolved for all samples except for the 4 MLs case. It can also be seen that the intensity, and thus the twinned volume, first decreases when the AlSb thickness increases between 1 and 4 MLs. The twinned volume then steadily increases with the AlSb thickness. This result highlights the strong influence of the AlSb nucleation layer thickness on the MT density, and the necessity to carefully adjust this parameter to optimize the material quality.

The ω-scans measured on this set of samples have already been described extensively elsewhere [12]. We reproduce here only the evolution of the full-width-at-half-maximum (FWHM) of the GaSb peak obtained for each sample from 004 ω-scans for sake of completeness. As can be seen on Fig. 3, the FWHM of the structures varies between about 650 and 950 arcsec, with a clear minimum value obtained for the structure comprising a 4 MLs thick AlSb nucleation layer. Similarly to what was observed in the pole figure measurements, the material quality first improves when increasing the AlSb thickness, but then steadily degrades for thicknesses larger than 4 MLs. This is further highlighted in Fig. 4 which plots the FWHM of the GaSb 004 diffraction peak versus the MT peak intensity from the pole figures. There is almost a linear dependence between these two material characteristics, which suggests that the twinned volume has a direct impact on the width of the diffraction peak. This contrasts significantly with what was observed at high temperature (500 °C): we have indeed demonstrated in a previous article that the FWHM at high temperature could be connected to the imperfections of the array of edge dislocations relieving the strain at the silicon substrate to antimonide material interface [12]. We have verified that this behavior is typical of the low temperature growth of the nucleation layer by comparing with samples having the same structure but where the AlSb was grown at 450 and 500 °C. The result obtained for 500 °C is shown in inset of Fig. 4. The trend seen at low temperature is not reproduced in that case: in a first step, the MT peak intensity decreases with increasing the AlSb thickness, but the FWHM is only slowly varying. On the contrary, between 17 and 50 MLs, the FWHM increases by about 100 arcsec while the MT intensity remains at a low level. Finally, the MT intensity increases drastically for the structure having a 150 MLs thick AlSb layer, while a minor FWHM difference with the sample with 50 MLs is noticed. This lack of any particular trend at 500 °C could also been observed at 450 °C, confirming that the relationship between the FWHM and the twinned volume is only valid at low temperature.